Journal of Global Change Data & Discovery. 2022, 6(2): 191-199
www.geodoi.ac.cn
©2022 GCdataPR
Global Change Research Data Publishing & Repository

A Satellite-Based Dataset of Global Atmospheric Carbon Dioxide Concentration with a Spatial Resolution of 2° × 2.5° from 1992 to 2020

Hou, W. Y.[1] Jin, J. X. [1,2*] Yan, T. [1] Liu, Y.[1]

1. College of Hydrology and Water Resources, Hohai University, Jiangsu, Nanjing 210024, China;
2. National Earth System Science Data Center, National Science & Technology Infrastructure of China, Beijing 100101, China

Abstract: Carbon dioxide (CO_2) is one of the main greenhouse gases in the atmosphere. It plays a crucial role in global climate change, of which temporal and spatial patterns have been paid great attention to. Taking CO_2 concentration as the research object, this study developed a global gridded dataset of monthly CO_2 concentration with a spatial resolution of 2° × 2.5° from 1992 to 2020. The time series of CO_2 concentration was simulated by an improved sinusoidal model, which was calibrated by the remotely-sensed product of tropospheric CO_2 concentration from 2002 to 2012 (AIR×3C2M 005), for each grid cell. Then, field-observed data of CO_2 concentration were adopted to evaluate the accuracy of our product. The results showed that: (1) the CO_2 concentration of our production was highly consistent with that observed at the stations. Especially, it performed well in the fitting (2002–2012: R^2 = 0.94, RMSE = 1.34 ppm), reconstruction (1992–2001: R^2 = 0.92, RMSE = 1.50 ppm) and prediction (2013–2019: R^2 = 0.93, RMSE = 1.58 ppm) of CO_2 concentration, respectively. (2) our data showed that the global atmospheric CO_2 concentration exhibited an obvious spatial heterogeneity. The high value regions of CO_2 concentration were mainly located in the northern of North America, while the low values dominated middle latitudes of the southern hemisphere.

Keywords: carbon dioxide; remote sensing; simulation; AIRS; global

DOI: https://doi.org/10.3974/geodp.20146.14.2022.02.04

CSTR: https://cstr.escience.org.cn/CSTR:20146.14.2022.02.04

Dataset Availability Statement:

The dataset supporting this paper was published and is accessible through the *Digital Journal of Global Change Data Repository* at: https://doi.org/10.3974/geodb.2021.11.01.V1 or https://cstr.escience.org.cn/CSTR:20146.11.2021.11.01.V1.

Received: 11-16-2021; **Accepted:** 12-31-2021; **Published:** 25-06-2022

Foundations: Ministry of Science and Technology of P. R. China (2018YFA0605402); National Natural Science Foundation (41971374)

***Corresponding Author:** Jin, J. X. ABE-5853-2021, Hohai University, National Earth System Science Data Center, National Science & Technology Infrastructure of China, jiaxinking@hhu.edu.cn

Data Citation: [1] Hou, W. Y., Jin, J. X., Yan, T. A satellite-based dataset of global atmospheric carbon dioxide concentration with a spatial resolution of 2° × 2.5° from 1992 to 2020 [J]. *Journal of Global Change Data & Discovery*, 2022, 6(2): 191–199. https://doi.org/10.3974/geodp.2022.02.04. https://cstr.escience.org.cn/CSTR:20146.14.2022.02.04.

[2] Hou, W. Y., Jin, J. X., Yan, T., *et al*. Global atmospheric carbon dioxide concentration simulation grid dataset (1992–2020) [J/DB/OL]. *Digital Journal of Global Change Data Repository*, 2021. https://doi.org/10.3974/geodb.2021.11.01.V1. https://cstr.escience.org.cn/CSTR:20146.11. 2021.11.01.V1.

1 Introduction

With the global economy development, a great deal of fossil fuels has been used which leads to a significant increase in carbon dioxide (CO_2) emissions. It has a great impact on the global climate, ecosystems and economic fields. The Intergovernmental Panel on Climate Change (IPCC) Fifth Assessment Report (AR5) states that CO_2 and methane are the main contributors to global warming (about 88%–90%)[1]. As an important greenhouse gas, the increase in the atmospheric concentration of CO_2 has a significant heating effect on the ground[2,3], which has attracted widespread attention from government departments and the scientific community. Exploring, retracing and predicting the changes of CO_2 concentration over the world are of great practical significance to adopt targeted policies and measures dealing with global climate change issues and achieving sustainable socio-economic developments.

Currently, there are three main ways to obtain CO_2 observations: ground-based, space-based and satellite remote sensing observations[4]. Data from ground-based stations have a large time span and high accuracy, which can be used as a benchmark for satellite observations. Many scholars used single-site data to represent the global CO_2 concentrations, which performed well in the studies. However, given the spatial heterogeneity of CO_2 distribution, single-site data was insufficient to present the truth on a global scale. In addition, ground observation stations are set up in sparsely populated and complex terrain. There are defects, e.g., the difficult construction, high cost of maintenance, small coverage, uneven distribution. Moreover, many sites are needed to cooperatively explore the regional dynamic change of CO_2[5,6]. Although CO_2 concentration can be measured with high accuracy, it had certain limitations for obtaining global CO_2 concentration data. Space-based exploration used aircraft or hot air balloons to make real-time high-altitude CO_2 concentration measurements in areas designated by the Earth System Research Laboratory (ESRL)[7,8]. Compared with site observations, CO_2 measurement data with a wider spatial coverage could be obtained through this method. However, due to the high cost of equipment and low timeliness, space-based detection could not acquire data continuously for a long time. Remote sensing uses diverse sensors on board satellites to acquire the spectral characteristics of atmospheric CO_2 which are radiated by the sun and reflected back into space through the ground. Tropospheric CO_2 observations with long-term, continuous, spatiotemporal consistency and high accuracy could be provided for continents and oceans[9]. This view has been widely accepted by the academic community. Currently, the atmospheric data provided by the Atmospheric Infrared Sounder (AIRS) have been adopted by many scholars in studies of atmospheric CO_2. With 2378 continuous infrared spectral channels (3.7–15.4 μm), the AIRS receives accurate infrared spectral data of land, ocean and atmosphere, and provides many hyperspectral and high-precision data including parameters of temperature, humidity, clouds, surfaces, and CO_2[10]. By comparing the AIRS data with the sounding observations, Divakarla et al. found that the relative error between land and sea did not exceed 10%[11]. Since the process of transporting surface CO_2 to the atmospheric troposphere one takes a few time, the data of AIRS inversion lags behind the real CO_2 concentration. Satellite CO_2 data products were derived from the near-infrared spectrum, in which they were strongly disturbed by surface atmospheric aerosols. This results in that global CO_2 data inversion by AIRS have a high degree of confidence only in the middle and lower layers of the troposphere[12]. It is urgent to develop a set of global-scale, longtime series, and high-precision CO_2 concentration data to support global change studies.

In these views, a new satellite-based dataset of global atmospheric CO_2 concentration was developed using an improved sinusoidal model in this study, including monthly and annual mean CO_2 concentration over the world. First, in order to ensure that satellite remote sensing data can accurately capture the concentration of tropospheric CO_2, the AIRS satellite remote sensing inversion data was validated by ground station observed data. Second, based on the improved sinusoidal model, the model was parameterized for each grid cell, and the global CO_2 simulation was carried out. The simulation results were evaluated by both site observations and satellite data, so that to provide reliable data of global CO_2 change.

2 Metadata of the Dataset

The metadata of the dataset [13] is summarized in Table 1. It includes the dataset full name, short name, authors, year of the dataset, temporal resolution, spatial resolution, data format, data size, data files, data publisher, and data sharing policy, etc.

Table 1 Metadata summary of the Global atmospheric carbon dioxide concentration simulation grid dataset (1992–2020)

Items	Description
Dataset full name	Global atmospheric carbon dioxide concentration simulation grid dataset (1992–2020)
Dataset short name	GlobalSimulatedCO2_1992–2020
Authors	Hou, W. Y. ABE-5925-2021, Hohai University, houhh5425@163.com Jin, J. X. ABE-5853-2021, Hohai University, jiaxinking@hhu.edu.cn Yan, T. ABE-5824-2021, Hohai University, 191309010014@hhu.edu.cn Liu, Y. ABE-5924-2021, Hohai University, 201301060011@hhu.edu.cn
Geographical region	60°S–88°N，180°W–180°E Year 1992–2020
Temporal resolution	Monthly CO_2 concentration from 1992 to 2020; annual mean CO_2 from 1992 to 2020
Spatial resolution	2° × 2.5° (Lat × Long) Data format NetCDF (.nc)
Data size	23.9 MB (After compression)
Data files	(1) Global monthly mean dataset of CO_2 concentrations during 1992–2020 (2) Global annual mean dataset of CO_2 concentrations during 1992–2020
Foundations	Ministry of Science and Technology of P. R. China (2018YFA0605402); National Natural Science Foundation (41971374)
Data publisher	Global Change Research Data Publishing & Repository, http://www.geodoi.ac.cn
Address	No. 11A, Datun Road, Chaoyang District, Beijing 100101, China
Data sharing policy	***Data*** from the Global Change Research Data Publishing & Repository includes metadata, datasets (in the *Digital Journal of Global Change Data Repository*), and publications (in the *Journal of Global Change Data & Discovery*). ***Data*** sharing policy includes: (1) ***Data*** are openly available and can be free downloaded via the Internet; (2) End users are encouraged to use ***Data*** subject to citation; (3) Users, who are by definition also value-added service providers, are welcome to redistribute ***Data*** subject to written permission from the GCdataPR Editorial Office and the issuance of a ***Data*** redistribution license; and (4) If ***Data*** are used to compile new datasets, the 'ten per cent principal' should be followed such that ***Data*** records utilized should not surpass 10% of the new dataset contents, while sources should be clearly noted in suitable places in the new dataset[14]
Communication and searchable system	DOI, CSTR, Crossref, DCI, CSCD, CNKI, SciEngine, WDS/ISC, GEOSS

3 Data Development Methodology

3.1 Data Sources

In this paper, the tropospheric CO_2 data product (AIRS × 3C2M005) jointly retrieved by AIRS and the Advanced Microwave Sounding Unit (AMSU) was used as the reference data

to produce the global CO_2 concentration dataset. AIRS/AMSU/HSB (the Humidity Sounder for Brazil) is a set of advanced atmospheric vertical profile observation instruments from infrared to microwave band, which is used to measure atmospheric temperature and provide information of atmospheric water vapor distribution, data of cloud, sea, land temperature and atmospheric humidity[15]. The adopted data was the third-level monthly average CO_2 data (version 5). The spatial coverage of the data is 60°S–90°N with a spatial resolution of 2° × 2.5° (latitude × longitude). The data was downloaded from the Goddard Earth Sciences Data and Information Services Center (GES DISC) of the National Aeronautics and Space Administration (NASA). In addition, the tropospheric CO_2 data product during 2010–2017 (AIRS3C2M 005) retrieved from AIRS was used to compare with the simulated data and site observations.

In our study, the AIRS remote sensing data and the products were evaluated by the monthly average CO_2 data of the stations. Seven sites were selected, namely Samoa (SMO), Mouna Loa (MLO), Variguan (WLG), Asserkrem (ASK), Niwot Ridge (NWR), Monte Cimone (CMN), and Plateau Rose (PRS) (Figure 1). The site data were obtained from the World Data Center for Greenhouse Gases (WDCGG). The global monthly average CO_2 data was downloaded from the Global Monitoring Laboratory of the National Oceanic and Atmospheric Administration (NOAA GML).

3.2 Algorithm Principle

The improved sinusoidal model[15] proposed by the Carbon Cycle Team of NOAA GML was adopted in this study. The model can reduce the noise generated from the process of estimating the global value due to atmospheric variability at the weather scale and measurement time gap.

The weekly air sample data from the global air sampling network[16] were used by Carbon Cycle Team of NOAA GML to calculate the global average surface value[17–20]. The samples came from the marine boundary layer (MBL) with well atmospheric mixing. The data could be estimated directly without the atmospheric transmission model, which captures the global trend with low noise. Global CO_2 concentration showed an upward trend and fluctuated with season. So, NOAA GML stakeholders chose a combination of quadratic functions and sine and cosine functions to represent suitably smooth curves for the MBL data. The specific parameters of the model vary with the gas type, site, and sampling frequency[15].The calculation formula is as follows:

$$f(t) = a_1 + a_2 t + a_3 t^2 + \sum_{k=1,4} [b_{2k-1} \sin(2\pi k t) + b_{2k} \cos(2\pi k t)] \quad (1)$$

where t denotes time. The model contains three polynomial parameters a_1, a_2, a_3, and eight sine and cosine harmonic parameters b_{2k-1} and b_{2k} (k = 1,2,3,4).

The model was applied to AIRS and AMSU satellite data products, and the consistency between the simulated data and satellite data was evaluated to ensure whether the model was also suitable. The AIRS and AMSU satellite data was input into the model, and the parameters were determined for each cell in the range of 60°S–88°N. Then, the simulation was performed to obtain the CO_2 concentration dataset pixel by pixel for this range. In order to analyze the interannual trend of CO_2 concentration from 1992 to 2020, the annual average growth trend of global CO_2 concentration was estimated by using Sen's slope estimator. That is, the median slope of all lines of paired points was selected as the slope overall. This

method could effectively calculate the change trend and reduce the uncertainty caused by outliers.

4 Data Results and Validation

4.1 Data description

The dataset mainly contents two subsets: (1) Global monthly mean CO_2 concentration dataset during 1992–2020, which includes 29 data files, named as CO2_mon_****.nc. (2) Global annual mean CO_2 concentration dataset during 1992–2020, which includes 29 data files, named as CO2_mean_****.nc.

4.2 Spatial and Temporal Variabilities of the CO_2 Concentration

The spatial distribution of the average CO_2 concentration data over the world from 1992 to 2020 is shown in Figure 1. Generally, the distribution of CO_2 exhibited an obvious spatial heterogeneity. The CO_2 concentration in the northern hemisphere was generally higher than that in the southern hemisphere. The areas with high CO_2 concentration were mainly distributed in northern North America, eastern Asia and low latitudes of the northern and southern hemispheres, while the areas with low CO_2 concentration were mainly distributed in the middle and high latitudes of the southern hemisphere and parts of Siberia.

Figure 2 shows the global pattern of the interannual trend of annual average CO_2 concentration from 1992 to 2020. Global CO_2 concentration is increasing, but the growth rate shows spatial heterogeneity. Overall, the growth rate of CO_2 concentration in the northern hemisphere was faster than that in the southern hemisphere. The CO_2 concentration in the high latitudes of the northern hemisphere, such as Siberia and northern North America, was increasing rapidly. In contrast, the areas with a slower rate were mainly located in the northern South America, central Africa and the low latitudes of the southern and northern hemispheres.

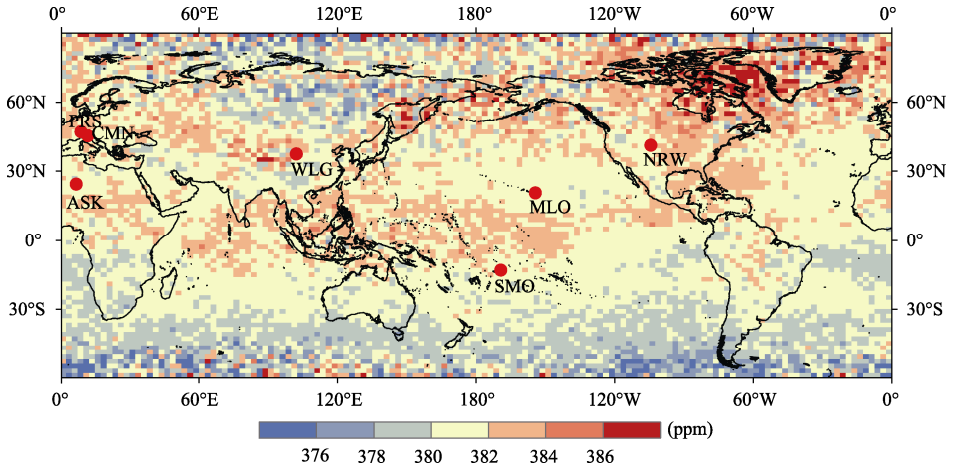

Figure 1 Spatial distribution of the multi-year mean CO_2 concentration from 1992 to 2020

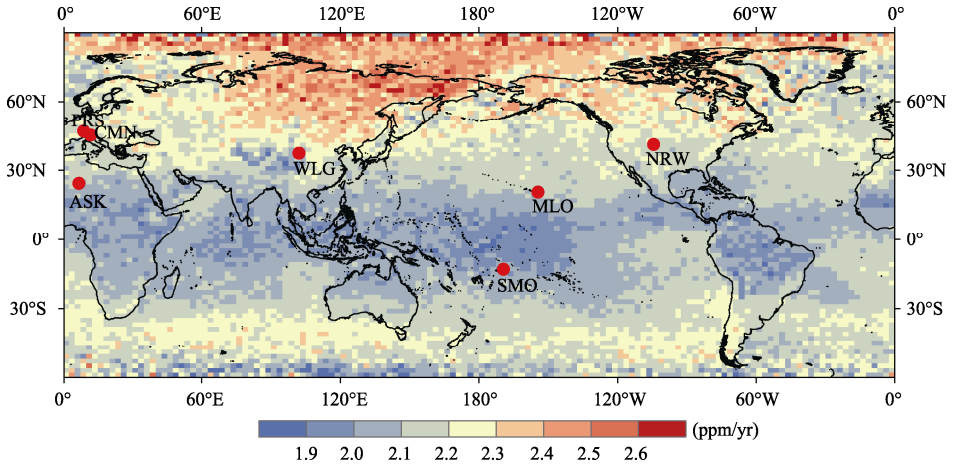

Figure 2 Spatial distribution of the trends in annual average CO_2 concentration from 1992 to 2020

4.3 Data Validation

4.3.1 Comparison of Fitting Results with Site Data

The simulation of CO_2 concentration in this study was compared with that from the seven stations from 1992 to 2019 (Figure 3). The result showed a significant linear relationship between them, indicating that the fitting results were well consistent with the concentration of CO_2 on the ground.

Performances of the proposed CO_2 concentration in this study were investigated in the reconstruction (1992–2001), fitting (2002–2012) and prediction (2013–2019) phases, respectively, including correlation coefficient, root mean square error (RMSE) and average relative error between the observed and simulated data at the seven stations (Table 2–4). The results showed that this dataset was well consistent with the observed CO_2 concentration on the ground in each phase. The error between the observed and simulated data in the fitting phase was the smallest, and RMSE was less than 5 ppm, which can well represent the ground CO_2 concentration.

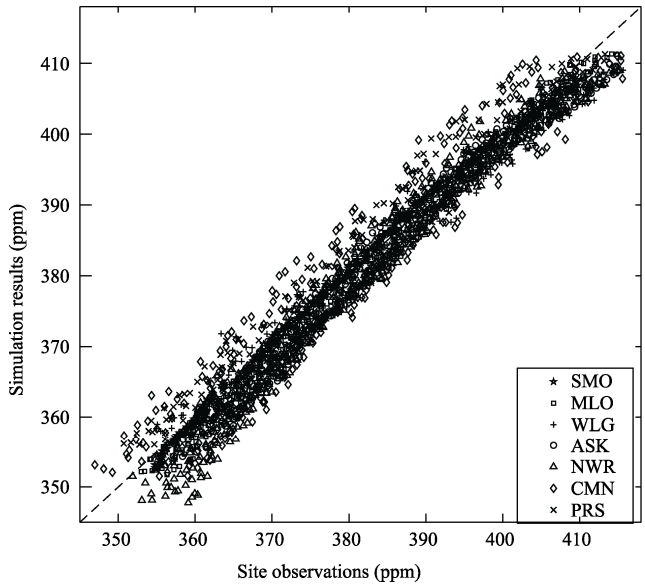

Figure 3 Comparison between the observed and simulated CO_2 concentration data at the seven stations

(Notes: SMO, Samoa; MLO, Mouna Loa; WLG, Variguan; ASK, Asserkrem; NWR, Niwot Ridge; CMN, Monte Cimone; PRS, Plateau Rose, and the same below.)

4.3.2 Comparison of Fitting Results, Satellite Data and Station Data

Three datasets of CO_2 concentration, i.e., the simulated data of this study, the AIRS product (2010.01–2017.02) and the site observations, were further compared using correlation coefficient (r), RMSE, relative error and R^2 at the seven stations. The results showed that the consistency between our simulated data and the observed data was generally better than that between the AIRS data and the observed data, indicating our dataset can well represent the real CO_2 concentration.

Table 2 Comparison between the observed and simulated monthly average CO_2 concentration in the reconstruction phase (1992–2001)

Site	Mean value (ppm)		Average deviation (ppm)	Correlation coefficient	RMSE (ppm)	Relative error
	Observed	Simulated				
SMO	362.88	362.78	0.10	0.994,4	0.91	0.20%
MLO	364.33	361.73	2.60	0.969,0	2.98	0.72%
WLG	365.86	362.96	2.90	0.845,8	2.71	0.63%
ASK	367.39	359.97	7.43	0.922,5	3.67	0.87%
NWR	364.78	360.58	4.20	0.913,4	5.22	1.22%
CMN	364.22	362.98	1.24	0.772,7	4.83	1.21%
PRS	364.65	363.64	1.02	0.877,7	2.94	0.69%

Table 3 Comparison between the observed and simulated monthly average CO_2 concentration in the simulation phase (2002–2012)

Site	Mean value (ppm)		Average deviation (ppm)	Correlation coefficient	RMSE (ppm)	Relative error
	Observed	Simulated				
SMO	381.79	382.70	–0.91	0.997,3	0.90	0.21%
MLO	383.66	382.00	1.66	0.970,6	2.21	0.49%
WLG	383.63	382.57	1.05	0.944,3	2.58	0.57%
ASK	383.42	382.78	0.64	0.954,7	1.99	0.46%
NWR	384.22	383.58	0.64	0.916,2	2.64	0.61%
CMN	383.23	384.22	–0.99	0.780,6	4.65	1.06%
PRS	383.69	383.78	–0.10	0.884,9	3.04	0.67%

Table 4 Comparison between the observed and simulated monthly average CO_2 concentration in the prediction phase (2013–2019)

Site	Mean Value (ppm)		Average deviation (ppm)	Correlation coefficient	RMSE (ppm)	Relative error
	Observed	Simulated				
SMO	400.63	399.92	0.70	0.996,1	1.39	0.28%
MLO	402.97	401.88	1.09	0.968,8	1.86	0.40%
WLG	402.99	400.44	2.55	0.925,0	3.68	0.78%
ASK	402.78	400.85	1.93	0.951,1	3.00	0.61%
NWR	403.43	401.91	1.52	0.898,8	3.31	0.71%
CMN	403.37	402.75	0.62	0.718,9	5.02	1.09%
PRS	401.35	403.87	–2.52	0.832,3	3.65	0.68%

5 Discussion and Summary

It was found that there may be a large deviation between the simulated and observed results. So, it is necessary to determine a starting point in order to ensure the good consistency between the backtracking results and the site observations. The growth trend of CO_2 in each region were generally consistent with that of the global average CO_2. Hence, the global average CO_2 (1980–2019) was used as the reference data. Since 1985, it had been calculated and compared as a segmentation point year by year. The time before and after the segmentation point was parameterized and simulated respectively, and then its results were compared consistently with the global average to ensure the highest accuracy. After inspection, when 1992 was taken as the segmentation point, the R^2 of the simulation was the highest (0.999,5) and RMSE was the lowest (0.451 ppm). Therefore, the year of 1992 was adopted as the starting year of this dataset.

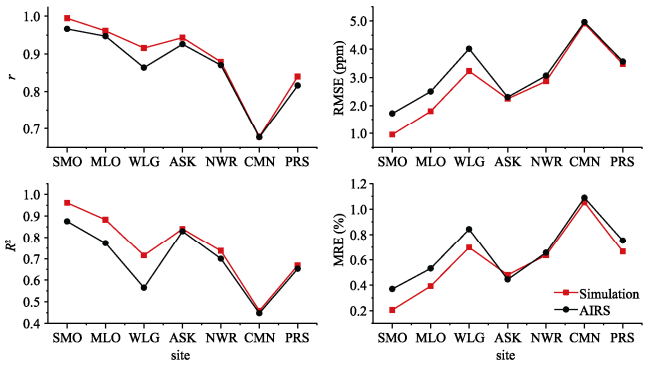

Figure 4 Comparison among the CO_2 concentration data derived from the simulated product of this study, satellite data products (AIRS) and site observations

The global tropospheric CO_2 concentration product jointly derived from AIRS and AMSU was used as reference data for parameter calibration of the improved sinusoidal estimation model and simulation of CO_2 concentration pixel by pixel. Then, field-observed data of CO_2 concentration were adopted to validate and evaluate the accuracy of our product. The dataset shows that the atmospheric CO_2 concentration exhibited an obvious spatial heterogeneity over the world. The high value regions of CO_2 concentration were mainly located in the middle and high latitudes of the northern hemisphere, and the low values dominated low latitudes of the southern hemisphere. Comparing the dataset with the site observation data, it is found that the two sets of data performed well in backtracking, simulation and prediction phases, which can well represent the spatio-temporal distribution global CO_2 in a long time series. Compared with the original satellite remote sensing data, this dataset can be used to study the change of atmospheric CO_2 concentration in a longer time series. Furthermore, it can improve the limitation that single-site numerical value was used to represent global CO_2 concentration in modeling at a global scale, and provide data support for studies of geography, ecology and other disciplines.

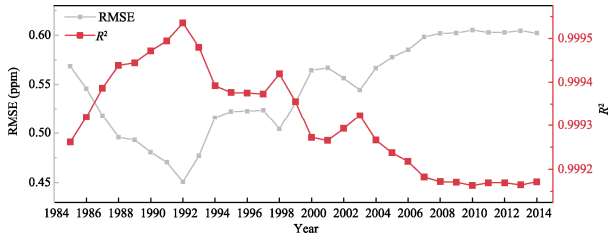

Figure 5 Comparison of consistency between simulation results and global observation data before and after different years as turning points

Author Contributions

Jin, J. X. made an overall design of this study; Hou, W. Y. collected and processed the data, and wrote the paper. Yan, T. wrote the codes. Liu, Y. verified the data of the paper.

Conflicts of Interest

The authors declare no conflicts of interest.

References

[1] Hartmann, D. L., Klein Tank, A. M. G., Rusticucci, M., *et al.* IPCC Climate Change 2013: The Physical Science Basis, Contribution of Working Group I to the Fifth Assessment Report of the Intergovernmental Panel on Climate Change [M]. Cambridge: Cambridge University Press, 2013.

[2] Callendar, G. S. The artificial production of carbon dioxide and its influence on temperature [J]. *Quarterly Journal of the Royal Meteorological Society*, 1938, 64(275): 223–240. DOI: 10.1002/qj.49706427503.

[3] Bacastow, R. B. The effect of temperature change of the warm surface waters of the oceans on atmospheric CO_2 [J]. *Global Biogeochemical Cycles*, 1996, 10(2): 319–333.

[4] Qianwen, M., Qiu Y. Remote sensing analysis of multi-years spatial and temporal variation of CO_2 in China [J]. *Remote Sensing Technology and Application*, 2016, 31(2): 203–213.

[5] Bergamaschi, P., Frankenberg, C., Meirink, J. F., *et al*. Inverse modeling of global and regional CH4 emissions using SCIAMACHY satellite retrievals [J]. *Journal of Geophysical Research*: *Atmospheres*, 2009, 114: D22301. DOI: 10.1029/2009JD012287.

[6] Shi, G. Y., Dai, T., Xu, N. Latest progress of the study of atmosphere CO_2 concentration retrievals from Satellite [J]. *Advances in Earth Science*, 2010 (1): 7–13.

[7] Menzel, W. P., Schmit, T. J., Zhang, P., *et al*. Satellite-based atmospheric infrared sounder development and applications [J]. *Bulletin of the American Meteorological Society*, 2018, 99(3): 583–603. DOI: 10.1175/BAMS-D-16-0293.1.

[8] Machida, T., Matsueda, H., Sawa, Y., *et al.* Worldwide measurements of atmospheric CO_2 and other trace gas species using commercial airlines [J]. *Journal of Atmospheric and Oceanic Technology*, 2008, 25(10): 1744–1754. DOI: 10.1175/2008JTECHA1082.1.

[9] Liu, Y., Lv, D. R., Chen, H. B., *et al*. Advances in technologies and methods for satellite remote sensing of atmospheric CO_2 [J]. *Remote Sensing Technology and Application*, 2011, 26(2): 247–254.

[10] Kuze, A., Suto, H., Nakajima, M., *et al*. Thermal and near infrared sensor for carbon observation Fourier-transform spectrometer on the Greenhouse Gases Observing Satellite for greenhouse gases monitoring [J]. *Applied optics*, 2009, 48(35): 6716–6733. DOI: 10.1364/AO.48.006716.

[11] Divakarla, M. G., Barnet, C. D., Goldberg, M. D., *et al*. Validation of Atmospheric Infrared Sounder temperature and water vapor retrievals with matched radiosonde measurements and forecasts [J]. *Journal of Geophysical Research*: *Atmospheres*, 2006, 111: D09S15. DOI: 10.1029/2005JD006116.

[12] Zhou, M. D. Atmospheric carbon dioxide (CO_2) retrieval and sensitivity studies from satellite observations [D]. Shanghai: East China Normal University, 2013.

[13] Hou, W. Y., Jin, J. X., Yan, T., *et al*. Global atmospheric carbon dioxide concentration simulation grid dataset (1992–2020) [J/DB/OL]. *Digital Journal of Global Change Data Repository*, 2021. https://doi.org/10.3974/geodb.2021.11.01.V1. https://cstr.escience.org.cn/CSTR:20146.11.2021.11.01.V1.

[14] GCdataPR Editorial Office. GCdataPR data sharing policy [OL]. https://doi.org/10.3974/dp.policy.2014.05 (Updated 2017).

[15] Thoning, K. W., P. P. Tans and W.D. Komhyr, Atmospheric Carbon Dioxide at Mauna Loa Observatory 2. Analysis of the NOAA GMCC Data, 1974–1985 [J]. *Journal of Geophysical Research*: *Atmospheres*, 1989, 94(D6): 8549–8565.

[16] Fetzer, E., Mcmillin, L. M., Tobin, D., *et al*. AIRS/AMSU/HSB validation [J]. *IEEE transactions on geoscience and remote sensing*, 2003, 41(2): 418–431. DOI:10.1109/TGRS.2002.808293.

[17] Conway, T. J., Tans, P. P., Waterman, L. S., *et al*. Evidence for interannual variability of the carbon cycle from the National Oceanic and Atmospheric Administration/Climate Monitoring and Diagnostics Laboratory global air sampling network [J]. *Journal of Geophysical Research*: *Atmospheres*, 1994, 99(D11): 22831–22855. DOI: 10.1029/94JD01951.

[18] Dlugokencky, E. J., Steele, L. P., Lang, P. M., *et al*. The growth rate and distribution of atmospheric methane [J]. *Journal of Geophysical Research*: *Atmospheres*, 1994, 99(D8): 17021–17043. DOI: 10.1029/94JD01245.

[19] Novelli, P. C., Steele, L. P., Tans, P. P. Mixing ratios of carbon monoxide in the troposphere [J]. *Journal of Geophysical Research: Atmospheres*, 1992, 97(D18): 20731–20750. DOI: 10.1029/92JD02010.

[20] Trolier, M., White, J. W. C., Tans, P. P., *et al*. Monitoring the isotopic composition of atmospheric CO2: Measurements from the NOAA Global Air Sampling Network [J]. *Journal of Geophysical Research: Atmospheres*, 1996, 101(D20): 25897–25916. DOI: 10.1029/96JD02363.